

**Impact of scar thickness on the assessment of viability using dobutamine
echocardiography and thallium single-photon emission computed tomography:
A comparison with contrast-enhanced magnetic resonance imaging**

Charles Nelson, Jane McCrohon, Frederick Khafagi, Stephen Rose, Rodel Leano,
and Thomas H. Marwick

J. Am. Coll. Cardiol. 2004;43;1248-1256

doi:10.1016/j.jacc.2003.09.062

This information is current as of April 8, 2011

The online version of this article, along with updated information and services, is
located on the World Wide Web at:

<http://content.onlinejacc.org/cgi/content/full/43/7/1248>

JACC

JOURNAL of the AMERICAN COLLEGE of CARDIOLOGY



Impact of Scar Thickness on the Assessment of Viability Using Dobutamine Echocardiography and Thallium Single-Photon Emission Computed Tomography

A Comparison With Contrast-Enhanced Magnetic Resonance Imaging

Charles Nelson, MBBS, FRACP, Jane McCrohon, MBBS, PhD, FRACP, Frederick Khafagi, MBBS, FRACP, Stephen Rose, PhD, Rodol Leano, BS, Thomas H. Marwick, MBBS, PhD, FACC

Brisbane, Australia

OBJECTIVES	We sought to determine whether the transmural extent of scar (TES) explains discordances between dobutamine echocardiography (DbE) and thallium single-photon emission computed tomography (TI-SPECT) in the detection of viable myocardium (VM).
BACKGROUND	Discrepancies between DbE and TI-SPECT are often attributed to differences between contractile reserve and membrane integrity, but may also reflect a disproportionate influence of nontransmural scar on thickening at DbE.
METHODS	Sixty patients (age 62 ± 12 years; 10 women and 50 men) with postinfarction left ventricular dysfunction underwent standard rest-late redistribution TI-SPECT and DbE. Viable myocardium was identified when dysfunctional segments showed TI activity $>60\%$ on the late-redistribution image or by low-dose augmentation at DbE. Contrast-enhanced magnetic resonance imaging (ceMRI) was used to divide TES into five groups: 0%, $<25\%$, 26% to 50%, 51% to 75%, and $>75\%$ of the wall thickness replaced by scar.
RESULTS	As TES increased, both the mean TI uptake and change in wall motion score decreased significantly (both $p < 0.001$). However, the presence of subendocardial scar was insufficient to prevent thickening; $>50\%$ of segments still showed contractile function with TES of 25% to 75%, although residual function was uncommon with TES $>75\%$. The relationship of both tests to increasing TES was similar, but TI-SPECT identified VM more frequently than DbE in all groups. Among segments without scar or with small amounts of scar ($<25\%$ TES), $>50\%$ were viable by SPECT.
CONCLUSIONS	Both contractile reserve and perfusion are sensitive to the extent of scar. However, contractile reserve may be impaired in the face of no or minor scar, and thickening may still occur with extensive scar. (J Am Coll Cardiol 2004;43:1248-56) © 2004 by the American College of Cardiology Foundation

Dobutamine echocardiography (DbE) and thallium single-photon emission computed tomography (TI-SPECT) remain the most widely available tests for the detection of viable myocardium (VM). Meta-analyses (1) and head-to-head comparisons (2,3) have shown TI-SPECT to be more sensitive but less specific for predicting functional recovery. These discordant results are often attributed to the investigation of different pathophysiologic processes with these tests—contractile reserve and membrane integrity.

Myocardial fibrosis has been shown to be an important contributor to the results of both tests and indeed is related to the likelihood of segmental recovery after revascularization (4,5). Discrepant results have been ascribed to the sensitivity of TI to small residua of VM in segments where scar prevents the thickening response to either DbE or revascularization (6). Conversely, lesser amounts of suben-

docardial scar may influence resting function and the DbE response; it has been suggested that resting systolic thickening is abolished by the transmural extent of scar (TES) $>20\%$ (7), and increasing TES may be associated with poorer contractile reserve (8). The ability to measure TES with contrast-enhanced magnetic resonance imaging (ceMRI) using delayed hyperenhancement after gadolinium injection (9) has enabled the direct evaluation of the effect of TES on contractile reserve and perfusion scintigraphy in humans.

Thus, we sought to observe the influence of TES on resting wall motion in order to determine its impact on the results of DbE and TI-SPECT in patients with left ventricular (LV) dysfunction and to identify whether discrepancies between TI-SPECT and DbE reflect TI uptake in subepicardial segments that are unable to cause wall thickening in response to Db.

METHODS

Patient selection. We studied 60 patients (age 61 ± 12 years; 50 men and 10 women) with LV dysfunction after

From the University of Queensland, Brisbane, Australia. This study was supported in part by a project grant (210217) from the National Health and Medical Research Council of Australia.

Manuscript received July 9, 2003; revised manuscript received August 16, 2003, accepted September 9, 2003.

Abbreviations and Acronyms

2DE	= two-dimensional echocardiogram/ echocardiographic
ceMRI	= contrast-enhanced magnetic resonance imaging
DbE	= dobutamine echocardiography
LV	= left ventricle/ventricular
TES	= transmural extent of scar
Tl-SPECT	= thallium single-photon emission computed tomography
VM	= viable myocardium

myocardial infarction (defined as ischemic chest pain with an appropriate rise in serum biochemical markers and/or electrocardiographic changes). Left ventricular dysfunction was evidenced by two or more segments showing abnormal wall motion on a pre-entry screening two-dimensional echocardiogram (2DE). Patients with coronary revascularization, valvular disease of more than moderate severity, end-stage renal failure, or any contraindication to DbE or MRI were excluded.

No patient had a clinical event between the time of the index infarction and the three viability studies. Contrast-enhanced MRI was performed after a median interval of 4.9 months after infarction. The viability studies were performed and interpreted independently at separate laboratories over a median interval of two weeks. All modalities were reported using a 16-segment model of the LV (10), with segments aligned in the transverse view using landmarks provided by the insertion of the right ventricle into the septum, as well as in the longitudinal view by the apex and base of the heart.

Dobutamine echocardiography. This test was performed using a standard Db/atropine protocol (11), with beta-adrenoceptor blocking drugs withheld on the day of the test. Dobutamine was infused at 5 $\mu\text{g}/\text{kg}$ per min and increased at 3-min intervals up to 40 $\mu\text{g}/\text{kg}$ per min; intermittent hand-grip and/or atropine (up to 2 mg intravenously) was employed if a maximum heart rate $<85\%$ beats/min was attained with DbE alone. Harmonic 2DE images were obtained using a commercially available machine (GE-Vingmed Vivid 5, Horten, Norway); this imaging was performed in five views and saved in digital format at baseline, low dose (5 and 10 $\mu\text{g}/\text{kg}$ per min), and peak, and the images were saved onto videotape at each stage. The images were interpreted by the consensus of two observers using the standard American Society of Echocardiography segmentation (10); segments were considered viable if they were dysfunctional at rest and had augmented function at low dose (5 to 10 $\mu\text{g}/\text{kg}$ per min).

Thallium SPECT. These studies were performed using a rest-late redistribution protocol (12). Patients were studied in the fasting state, with the initial images performed 20 to 30 min after injection of 150 MBq of Tl-201 at rest, and redistribution images performed 17 to 24 h after the initial

injection. Images were obtained on a GE Optima dual-head gamma camera (GE Medical Systems, Milwaukee, Wisconsin) fitted with low-energy, all-purpose, parallel-hole collimators and interfaced to acquisition and processing computers. Sixty-four views were obtained in a semicircular orbit from the right anterior oblique to the left posterior oblique projections, and tomograms were reconstructed using filtered back-projection and displayed as short-axis and horizontal and vertical long-axis slices and as quantitative polar maps. Segmental Tl uptake was assessed visually for redistribution and was quantified as a proportion of maximum counts on the redistribution image. Data were not corrected for scatter or attenuation. Segments with a resting wall motion abnormality on 2DE were designated as viable if activity was $>60\%$ of maximum (13) or showed significant redistribution. When Tl activity varied within a given segment, the Tl activity was assessed in the site analogous to the echocardiographic imaging plane.

Contrast-enhanced MRI. Cardiac magnetic resonance images were obtained using a Sonata 1.5-T scanner (Siemens, Erlangen, Germany). Left ventricular anatomy and function images were acquired in horizontal and vertical long-axis views (four- and two-chamber equivalent views), as well as in six to eight short-axis views using true free induction, steady-state precession (FISP) imaging (14,15) during breath-hold. First-pass images were obtained immediately after injection of 0.1 mmol/kg gadolinium (Gadoversetamide, Mallinkrodt, St. Louis, Missouri). Contrast-enhanced images were obtained using an inversion-recovery segmented gradient echo sequence, with a voxel size of $1.7 \times 1.4 \times 8$ mm, adjusting the inversion times (260 to 400 ms) to nullify signal from the normal myocardium. Imaging was started 5 min after infusion and completed 12 ± 4 min later. Image acquisition and analysis followed the protocol described by Kim et al. (9). The selection of images for interpretation was based on the superiority of scar delineation at an average of 9 ± 2 min.

An expert reader, blinded to other data, separately interpreted wall motion on MRI using the same segmentation and scoring scale as used for echocardiography. This observer also independently interpreted TES into five categories: no scar; 1% to 25%; 26% to 50%, 51% to 75%, and 75% to 100%, guided by quantification of scar thickness and myocardial thickness (Efilm, Merge, Milwaukee, Wisconsin). Thickening was also measured in each segment. When TES varied within a given segment, the category was assessed in the site analogous to the echocardiographic imaging plane. In order to permit a binary distinction of ceMRI into viable and nonviable for comparison with SPECT and DbE data, segments with $<50\%$ scar were designated as viable and those with $>50\%$ scar as nonviable.

Statistical analysis. Data are expressed as the mean value \pm SD. The Student *t* test or chi-square test was used to compare the difference between two groups. Kappa statistics were used to characterize the level of agreement in the distinction of viable from nonviable myocardium with ceMRI, SPECT, and DbE. Differences between the five groups of TES with respect

to SPECT and DbE results were assessed using one-way analysis of variance with Bonferroni's post hoc test. A general linear model was used to investigate the association of TES with scar by DbE, scar by SPECT, and the interaction between these terms. Data were analyzed using standard statistical software (SPSS, Chicago, Illinois). A p value <0.05 was considered statistically significant.

RESULTS

Patient characteristics. The clinical details are shown in Table 1. We selected patients with LV dysfunction after infarction, and of the study group, only 52% had undergone thrombolysis and none had undergone primary angioplasty. The infarct size was significant, as evidenced by an average creatine kinase level of >2,000 U/l, and selected patients were significantly limited by LV dysfunction, the majority being in functional class II for dyspnea (47%), with a mean exercise capacity of 5 METs.

Table 2 summarizes the main findings by 2DE and MRI on a per patient basis. The median number of segments with abnormal wall motion was five for both 2DE and MRI.

Segments showing abnormal function or scar by MRI. There were 360 segments that were assessed as abnormal on the basis of ceMRI evidence of scar, or as having abnormal function by MRI. A comparison between MRI and echocardiographic wall motion is illustrated in Table 3. Segmental thinning (defined by thickness <6 mm by MRI) was present in only 28 segments showing resting dysfunction (8%).

Relationship of TES to resting function by MRI and echocardiography. We compared TES with resting function in 382 segments identified as showing abnormal function by either resting echocardiography or MRI (Fig. 1). For both MRI and 2DE, as TES increased, there was a significant

Table 1. Clinical Characteristics of Patients (n = 60)

Age (yrs)	61 ± 10
Male gender	50 (83%)
Infarct characteristics	
Troponin (µg/l)	24 ± 37
Creatine kinase (U/l)	2,045 ± 2,035
Anterior or septal ST-segment elevation	22 (37%)
Inferior, posterior, or lateral ST-segment elevation	20 (33%)
Non-ST-segment elevation pattern	18 (30%)
Multiple myocardial infarctions	14 (23%)
Clinical status	
NYHA functional class	2 ± 1
Exercise capacity (METs)	5 ± 2
Drug therapy	
Beta-adrenoceptor blockers	87%
ACE inhibitor or A ₂ receptor blocker	73%
Testing after myocardial infarction	
1-3 months	18 (30%)
3-6 months	16 (27%)
>6 months	26 (43%)

Data are presented as the mean value ± SD or number (%) of patients.
A₂ = angiotensin II; ACE = angiotensin-converting enzyme; METs = metabolic equivalents; NYHA = New York Heart Association.

Table 2. Characteristics of Imaging in 60 Patients With Left Ventricular Dysfunction

Echocardiography	
Ejection fraction (%)	40 ± 10
Abnormal wall motion in	
<4 segments	19 (32%)
4-8 segments	24 (40%)
≥8 segments	17 (28%)
Magnetic resonance imaging	
Ejection fraction (%)	43 ± 11
Abnormal wall motion in	
<4 segments	17 (28%)
4-8 segments	28 (47%)
≥8 segments	15 (25%)
Contrast enhancement in	
<4 segments	22 (37%)
4-8 segments	32 (53%)
≥8 segments	6 (10%)

Data are presented as the mean value ± SD or number (%) of patients.

reduction in the proportion of segments that retained some contractile function. Nonetheless, the presence of scar in the subendocardium was insufficient to prevent thickening, with >50% of segments in the 25% to 75% TES range still having some contractile function at rest, although almost all segments with >75% scar had abnormal resting function.

Relationship between viability and TES. Figure 2 shows the relationship between viability and TES in 382 segments identified as showing abnormal function by either resting echocardiography or MRI. As TES increased, both mean TI uptake (r = -0.49, p < 0.0001) and change in wall motion score decreased significantly (r = -0.20, p < 0.0001). Similarly, as TES increased, the proportion of segments designated as viable by either DbE or TI-SPECT significantly decreased, and the relationship of both tests to increasing TES was similar. The same relationship between TES and the proportion of segments viable by either DbE or TI-SPECT was detected in akinetic and hypokinetic segments.

Segmental concordance. A segmental comparison between the techniques is illustrated in Figure 3. As we were particularly interested in understanding the correlates of the DbE response, we analyzed the viability responses of 372 segments with abnormal resting function by echocardiography (Fig. 4). There was fair agreement between DbE and TI-SPECT, as well as moderate agreement when each test was compared with the presence or absence of viability by ceMRI. The correlation between DbE and ceMRI was similar, irrespective of the time since infarction (remembering that early infarcts were not represented, as patients entered the study after a minimum interval of 1 month after infarction).

Concordance between DbE and TI-SPECT. Figure 5 summarizes the proportion of segments in which the results of TI-SPECT and DbE were concordant (i.e., either viable by both tests or nonviable by both tests) in each category of TES. The overall concordance between TI-SPECT and DbE increased with increasing TES, reaching 80% concor-

Table 3. Characteristics of Abnormal Segments by Magnetic Resonance Imaging (Showing Regional Dysfunction or Gadolinium Late Enhancement)

	n	Thickening (mm)	Thickening (%)	ceMRI	Echocardiographic Score		
					Normal	Hypokinetic	Akinetic
Normal	30	3.8 ± 2.4	47 ± 40	0.8 ± 0.9	21 (70%)	9 (30%)	0
Hypokinetic	205	2.1 ± 2.0	28 ± 29	1.4 ± 1.4	33 (16%)	106 (52%)	66 (32%)
Akinetic	125	1.1 ± 2.0	16 ± 29	2.5 ± 1.5	10 (8%)	28 (22%)	87 (70%)

Data are presented as the number (%) of segments or mean value ± SD.
 ceMRI = contrast-enhanced magnetic resonance imaging.

dance with TES >75%. There was a significant association between concordance of DbE and TI-SPECT and increasing TES ($p < 0.0001$). Almost 80% of segments without scar that are viable by DbE are viable by TI-SPECT, with more discrepancies with increasing TES ($p = 0.03$). Segments that are nonviable by DbE show increasing concordance with increasing TES ($p < 0.0001$) and were the most discordant in the absence of scar. However, in the TES >75% category, 16 of the 68 segments were viable by SPECT and eight by DbE, implying that SPECT does not excessively identify viability in segments where there is a thin rim of residual viable tissue.

DISCUSSION

This study reports, for the first time, the impact of TES (measured noninvasively rather than with biopsy) on resting function, contractile reserve, and relative perfusion. The results show that although increasing TES is associated with a significant reduction in the proportion of segments showing residual contractile function, over 50% of segments still

showed some contractile function in the presence of TES ranging from 25% to 75%, even though almost all segments with >75% scar had abnormal resting function. Finally, TI-SPECT identified <25% of the 68 segments in the 76% to 100% TES category as viable, suggesting that TI-SPECT does not excessively identify viability in segments where there is only a thin rim of residual viable tissue.

Discrepancies between MRI and DbE. The results of this study show a moderate concordance between the categorical diagnosis of scar by ceMRI and contractile reserve.

CONTRIBUTION OF SUBENDOCARDIAL SCAR TO RESTING FUNCTION. A number of biopsy studies have demonstrated that the presence of contractile reserve and the amount of tracer uptake within segments—and, indeed, the likelihood of functional recovery—are related to the amount of fibrosis within the segment (4,5). The presence of >20% fibrosis is associated with technetium-99m sestamibi uptake <55% of maximum (5). What has been unclear, however, is the importance of the site of myocardial scar with respect to the presence of residual contraction.

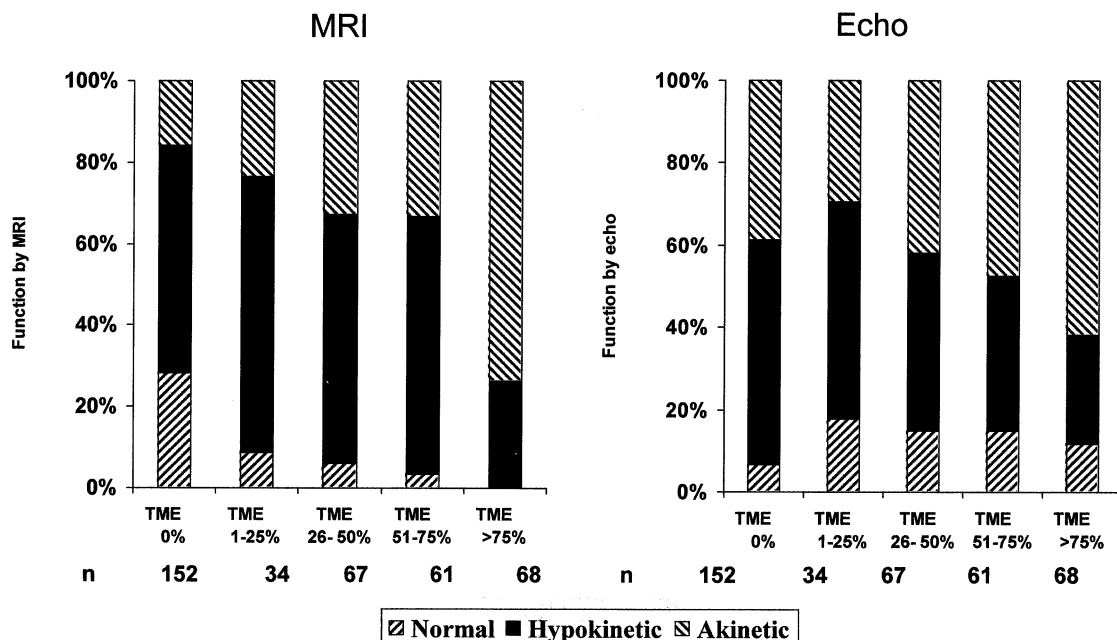


Figure 1. Relationship between transmurular extent of scar (TES) and resting systolic function by magnetic resonance imaging (MRI) (left) and two-dimensional echocardiogram (2DE) (right). Increasing TES is associated with a significant reduction in the proportion of segments with residual wall thickening ($p < 0.001$ for both MRI and 2DE). Note that in the 25% to 75% TES range, over 50% of segments still have some contractile function at rest, whereas almost all segments with >75% scar have abnormal resting function.

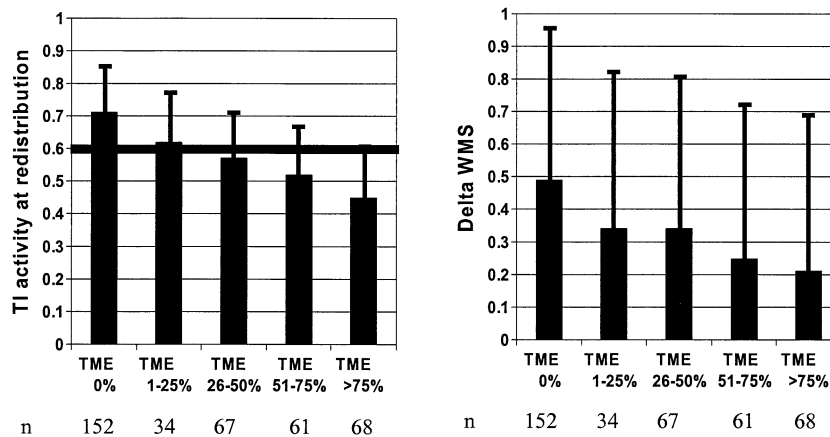


Figure 2. Relationship between transmurality extent of scar (TES) and thallium (Tl) activity at late redistribution (**left**) and increase in wall motion score (WMS) with low-dose dobutamine (**right**). Thallium activity at redistribution and the degree of low-dose augmentation both decrease significantly with increasing TES ($p < 0.001$), with no significant difference between dobutamine echocardiography and Tl-single-photon emission computed tomography. The 60% Tl activity cut-off for viability is shown.

In a dog model of acute infarction, Lieberman et al. (7) demonstrated a loss of resting systolic thickening with a transmural extent of infarction of $>20\%$. Similarly, a study using MRI tagging demonstrated that circumferential shortening and maximal shortening were reduced uniformly across the wall in both transmural and nontransmural infarcts (16). Although widely extrapolated to human physiology, these data may be influenced by the acute nature of the models, which do not account for the contribution of stunning or hibernation to resting wall motion abnormalities (17). Other dog models have shown fractional contributions to total wall thickening of the inner, middle, and outer thirds of the myocardial wall to be 58%, 25%, and 17%, respectively, indicating a 2:1 contribution of the inner to outer half to wall thickening (18), similar to the 71% to 29% contribution of the inner and outer halves as reported by Gallagher et al. (19).

In contrast to these data, this study of chronic coronary disease in humans indicates that some contractile function persists in 50% of segments where TES ranges from 25% to 100%. These findings are consistent with a comparison of ceMRI and wall motion presented by Wu et al. (20). Among 250 segments with hyperenhancement in that study, 62 (25%) had normal wall motion, the majority with scar involving $<50\%$ of the thickness of the wall. Although it is likely that MRI detection of wall motion abnormality is more accurate than 2DE, because of superior spatial resolution (21) and better assessment of wall thickening and thinning by excellent visualization of the epicardial borders (22), wall motion abnormalities were detected to a similar degree with both MRI and echocardiography.

CONTRIBUTION OF SUBENDOCARDIAL SCAR TO CONTRACTILE RESERVE. Previous work has indicated that the Db response reflected the total extent of scar (4). Our results are in broad agreement with these findings, showing that both the change in wall motion score between rest and low-dose Db (Fig. 2) and the number of DbE-viable segments (Fig.

5) are markedly reduced by more extensive scar ($>50\%$ of LV wall). Although the presence of subendocardial scar is considered to be less important to the response to Db than to resting function, it is thought to be responsible for the lack of specificity of DbE in the distinction between viable segments and nontransmural scar. Moreover, the TES is only one of a number of determinants of loss of contractile reserve; discordance between DbE and Tl-SPECT was greatest in segments with no contractile reserve and no scar, as 62% of such segments were viable by SPECT. One potential contributor is the presence of ischemia—in the absence of revascularization, Db-induced ischemia could certainly impede the augmentation response, although induction at a low dose is considered to be uncommon.

Discrepancies between MRI and Tl-SPECT. The prediction of myocardial viability with Tl-SPECT is inversely related to the amount of scar tissue in the wall, which determines the likelihood of recovery after revascularization (5). The importance of the amount of scar to Tl activity is emphasized in Figure 2, where the relationship appears rather stronger than with DbE. However, in the setting of limited ($\leq 25\%$) subendocardial scar, the MRI technique is more sensitive than SPECT, with 50% of segments with and without contractile reserve showing viability by SPECT criteria. These data reinforce the findings of the only previous study of ceMRI and SPECT in 91 patients with known or suspected coronary artery disease, which showed that although both tests identified all segments with nearly transmural infarction, ceMRI identified subendocardial infarcts missed by SPECT (23).

Understanding discrepancies between DbE and Tl-SPECT. Although viability is obviously a continuum, decision-making is necessarily binary, so the comparison of the techniques (Fig. 4) is unavoidable. The concordance between these studies was only modest and matches some previous comparisons between SPECT and echocardiographic techniques. Although DbE and Tl-SPECT are

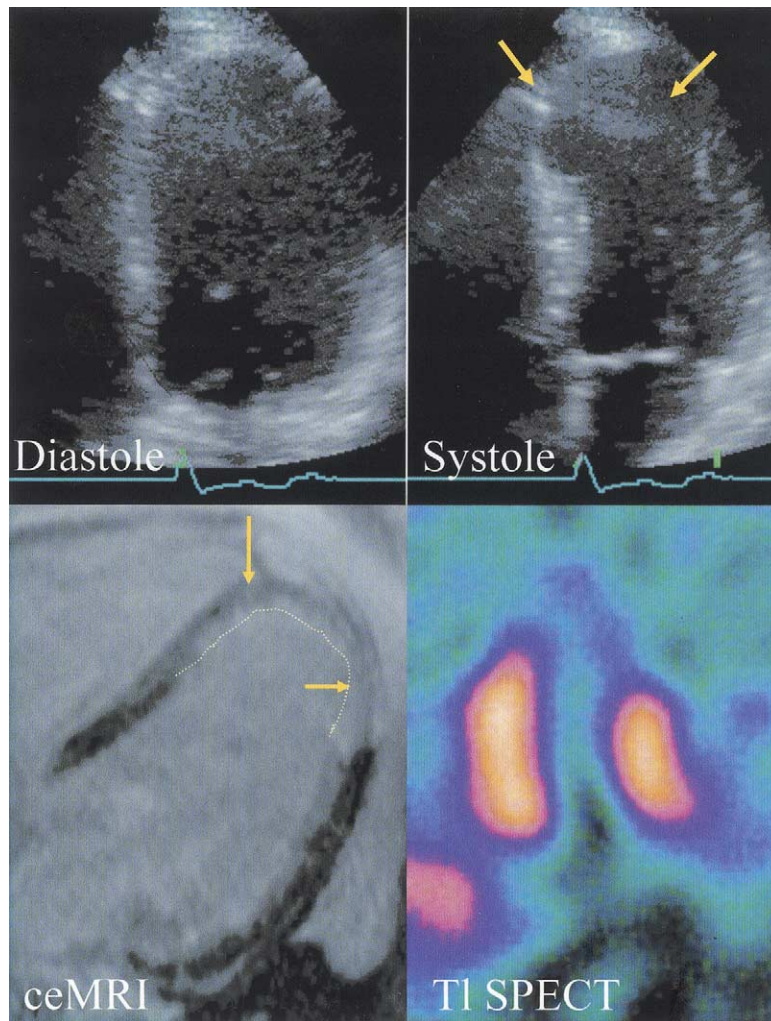


Figure 3. Correlation between dobutamine echocardiography and thallium single-photon emission computed tomography (TI-SPECT) in a patient demonstrating nontransmural infarction in the apical septum (**long arrow**) and transmural infarction of the apical lateral segment (**short arrow**) by contrast-enhanced magnetic resonance imaging (ceMRI). The resting echocardiogram shows akinesia of both segments, and TI-SPECT shows a severe perfusion defect.

widely used for the identification of VM, the aspects of viability that they identify are fundamentally different, so that discordances are to be anticipated. Our finding of moderate agreement ($\kappa = 0.24$) was within the range of existing comparisons of DbE and TI-SPECT. Although there are some variations in the literature, some previous comparisons of DbE and TI-SPECT have shown agreement in only 60% of segments (24), analogous to the findings of this study. Kappa values have ranged from 0.49 to 0.56 in studies with high concordance (6,25), whereas others have shown much lower values (from 0.09 to 0.12) (2). The potential sources of variation are numerous and include the exact methodologies used (e.g., rest vs. stress SPECT, low-dose vs. full-dose DbE), the thresholds for identifying viability (e.g., threshold for interpreting contractile reserve, threshold of Tl activity used to identify viability), a loss of contractile reserve response due to severely reduced flow, and the presence of severe myocyte damage with a loss of contractile apparatus. The topics that warrant

specific discussion are matters relating to image orientation and TES.

A perennial challenge to comparative imaging studies includes the difficulty posed by matching up of segments to ensure that the exact same piece of myocardium was being compared across all three modalities. This is more problematic with 2DE than with the two other techniques, where slice alignment in the heart can be controlled during the acquisition or post-processing. King *et al.* (26) have shown that 2DE planes often deviate from the expected axes, so that the discrepancies in Figure 4 may partly reflect the interpretation of different pieces of myocardium, and the lower kappa values than with TI-SPECT are likely consistent with limitation. Nonetheless, despite this limitation of 2DE, it has a large pool of literature of comparative tests with other modalities, it remains the most widely applied approach for wall motion analysis, and an understanding of its relationship with TES is important to better understand the technique. As in our previous experience of such compar-

All	ceMRI				ceMRI				DbE						
			NV	V			NV	V			NV	V			
	TI SPECT	NV	97	97	194	DbE	NV	104	127	231	TI SPECT	NV	143	51	194
		V	32	146	178		V	25	116	141		V	88	90	178
		129	243	372			129	243	372			231	141	372	
	Kappa = 0.32				Kappa = 0.24				Kappa = 0.24						
≤3 months	ceMRI				ceMRI				DbE						
			NV	V			NV	V			NV	V			
	TI SPECT	NV	20	38	58	DbE	NV	22	35	57	TI SPECT	NV	34	24	58
		V	12	51	63		V	10	54	64		V	23	40	63
		32	89	121			32	89	121			57	64	121	
	Kappa = 0.16				Kappa = 0.24				Kappa = 0.22						
>3 months	ceMRI				ceMRI				DbE						
			NV	V			NV	V			NV	V			
	TI SPECT	NV	77	59	136	DbE	NV	82	92	174	TI SPECT	NV	109	27	136
		V	20	95	115		V	15	62	77		V	65	50	115
		97	154	251			97	154	251			174	77	251	
	Kappa = 0.38				Kappa = 0.22				Kappa = 0.24						

Figure 4. Pairwise agreement in the diagnosis of segments as viable (V) and nonviable (NV) with dobutamine echocardiography (DbE), contrast-enhanced magnetic resonance imaging (ceMRI), and thallium single-photon emission computed tomography (TI-SPECT). The **top row** relates to the correspondence in all 372 segments, whereas the **middle and bottom rows** reflect the agreement in patients studied ≤3 months and >3 months after infarction. Each modality demonstrated only moderate agreement with the other two, irrespective of the time since infarction.

isons, we sought to minimize discrepancies by using standard anatomic landmarks to localize segments and using the same 16-segment echocardiography model (10) for each test.

Several authors have proposed that TI-SPECT requires lesser amounts of live tissue than DbE to detect viability (6). Although the current study is consistent with this observation, the total number of discrepancies is small in the TES >75% category, with 16 segments viable by SPECT and eight viable by DbE.

As noted by Panza et al. (27), disagreement between the two tests was related primarily to segments considered viable by TI that did not show contractile improvement with Db. However, while the former study speculated that one of the possible mechanisms was a greater extent of myocardial necrosis in these regions compared with those with a positive response to Db, the current study confirms that this is indeed the mechanism. Indeed, the close relationship of discrepancies to TES suggests that other postulated mechanisms, including a reduction of blood flow insufficient to maintain a positive response to Db but sufficient to maintain transmembrane pump function, or more frequent episodes

of ischemia leading to a more severe form of chronic myocardial “stunning,” may be less important.

Interestingly, the number of segments identified as nonviable by SPECT and DbE, but not by ceMRI, exceeds the number of disagreements between SPECT and DbE. This discrepancy between MRI and the other tests likely reflects the viability (or lack thereof) of the remainder of the wall—for example, <50% TES may be identified as nonviable by SPECT if flow is reduced to the remainder of the wall, or by DbE if the rest of the wall lacks contractile reserve. Thus, despite the respective favorable and unfavorable implications of subendocardial and transmural scar extent with ceMRI (9), the discrepancies with other functional tests may have important implications, especially in segments with intermediate scar thickness, where the functional outcome may be determined by the nature of the tissue in the rest of the wall.

Study limitations. This investigation compared the results of viability studies to TES, in the belief that this is the best standard for necrosis, if not for viability. An alternate approach would be to compare the results with the presence

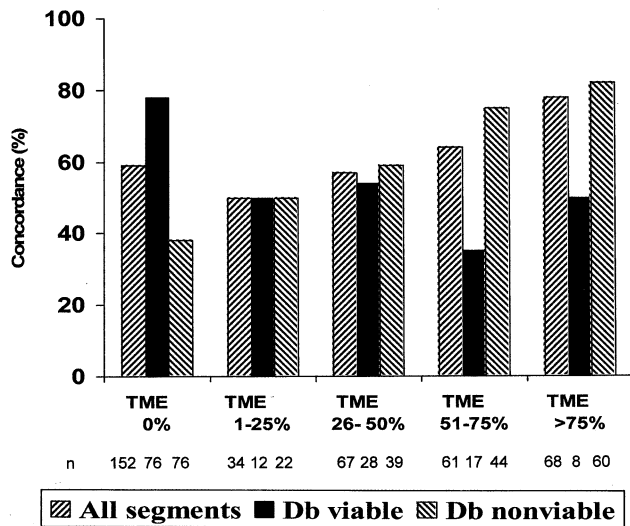


Figure 5. Proportion of segments in which the results of thallium single-photon emission computed tomography (TI-SPECT) and dobutamine echocardiography (DbE) were concordant (viable by both tests or nonviable by both tests) in each category of transmural extent of scar (TES). The overall concordance between TI-SPECT and DbE is similar in each category of TES, increasing with TES >75%. Most segments that are viable by DbE are viable by TI-SPECT when there is no scar (i.e., TES 0%), with more discrepancies as TES increases ($p = 0.03$). Segments that are nonviable by DbE show increasing concordance with increasing TES ($p < 0.0001$).

or absence of recovery of contractile function after revascularization. Although widely used to document the reliability of these modalities (3,9), this remains an unconvincing “gold standard” on several counts. First, the decision to revascularize introduces potential selection bias. Second, the time course of functional recovery of hibernating segments may be up to 14 months (28), a length of follow-up that has rarely been adhered to, with the risks of interim changes due to restenosis, graft closure, new plaque rupture, and remodeling (29). Third, revascularization of VM has or may have benefits other than recovery of resting contractile function, such as recovery of contractile function in response to stress, prevention or even reversal of remodeling, symptom control, improved exercise tolerance, prevention of arrhythmias and arrhythmic death, and ultimately prolongation of survival.

The timing of studies is a potential source of variation. It is possible for areas of myocardium to move between the normal, stunned, and hibernating categories, but the presence of a differential change between different TES categories seems unlikely. We excluded patients with acute infarction, because previous pathologic and MRI studies have shown infarcts to shrink approximately fourfold between four days and six weeks (30,31). However, because our patients were imaged at a median interval of almost five months after myocardial infarction, it is likely that the bulk of infarct shrinkage had already occurred; indeed, the relationship between viable and nonviable responses (Fig. 4) showed minimal variation based on the time after infarction.

Finally, the cMRI protocol used in this study involved imaging at an average of 9 min after injection of gadolinium.

Although the importance of this timing in patients late after infarction is disputed, some investigators have imaged after a minimum of 10 min. It is conceivable that this may have influenced the assessment of TES in this study.

Conclusions. The likelihood of residual contractile function decreases with increasing TES, but residual function is seen in many segments with >25% TES. The reduction of contractile reserve and TI activity is comparable with increasing transmural extent. Transmural extent is a determinant of discordance between the two tests, but discordance is greatest in segments with no contractile reserve and transmural extent of 0% to 25%, whereas TI uptake within small areas of subepicardial viable tissue does not appear to explain many discrepancies between DbE and TI-SPECT assessment of myocardial viability.

Acknowledgments

The authors gratefully acknowledge the support of the Centre for Advanced MRI, Wesley Hospital, Brisbane, Australia, where the MRI data were acquired.

Reprint requests and correspondence: Prof. Thomas H. Marwick, University of Queensland Department of Medicine, Princess Alexandra Hospital, Ipswich Road, Brisbane, Qld 4012, Australia. E-mail: tmarwick@soms.uq.edu.au.

REFERENCES

- Bax JJ, Wijns W, Cornel JH, Visser FC, Boersma E, Fioretti PM. Accuracy of currently available techniques for prediction of functional recovery after revascularization in patients with left ventricular dysfunction due to chronic coronary artery disease: comparison of pooled data. *J Am Coll Cardiol* 1997;30:1451-60.
- Perrone-Filardi P, Pace L, Prastaro M, et al. Assessment of myocardial viability in patients with chronic coronary artery disease: rest-4-hour-24-hour ^{201}Tl tomography versus dobutamine echocardiography. *Circulation* 1996;94:2712-9.
- Vanoverschelde JL, D'Hondt AM, Marwick T, et al. Head-to-head comparison of exercise-redistribution-reinjection thallium single-photon emission computed tomography and low dose dobutamine echocardiography for prediction of reversibility of chronic left ventricular ischemic dysfunction. *J Am Coll Cardiol* 1996;28:432-42.
- Shan K, Bick RJ, Poindexter BJ, et al. Altered adrenergic receptor density in myocardial hibernation in humans: a possible mechanism of depressed myocardial function. *Circulation* 2000;102:2599-606.
- Dakik HA, Howell JF, Lawrie GM, et al. Assessment of myocardial viability with $^{99\text{m}}\text{Tc}$ -sestamibi tomography before coronary bypass graft surgery: correlation with histopathology and postoperative improvement in cardiac function. *Circulation* 1997;96:2892-8.
- Zamorano J, Delgado J, Almeria C, et al. Reason for discrepancies in identifying myocardial viability by thallium-201 redistribution, magnetic resonance imaging, and dobutamine echocardiography. *Am J Cardiol* 2002;90:455-9.
- Lieberman AN, Weiss JL, Jugdutt BI, et al. Two-dimensional echocardiography and infarct size: relationship of regional wall motion and thickening to the extent of myocardial infarction in the dog. *Circulation* 1981;63:739-46.
- Armstrong WF. 'Hibernating' myocardium: asleep or part dead? *J Am Coll Cardiol* 1996;28:530-5.
- Kim RJ, Wu E, Rafael A, et al. The use of contrast-enhanced magnetic resonance imaging to identify reversible myocardial dysfunction. *N Engl J Med* 2000;343:1445-53.
- Armstrong WF, Pellikka PA, Ryan T, Crouse L, Zoghbi WA. Stress echocardiography: recommendations for performance and interpretation of stress echocardiography. Stress Echocardiography Task Force of the Nomenclature and Standards Committee of the American

- Society of Echocardiography. *J Am Soc Echocardiogr* 1998;11:97–104.
11. Geleijnse ML, Fioretti PM, Roelandt JR. Methodology, feasibility, safety and diagnostic accuracy of dobutamine stress echocardiography. *J Am Coll Cardiol* 1997;30:595–606.
 12. Dilsizian V, Bonow RO. Current diagnostic techniques of assessing myocardial viability in patients with hibernating and stunned myocardium. *Circulation* 1993;87:1–20.
 13. Udelson JE, Coleman PS, Metherall J, et al. Predicting recovery of severe regional ventricular dysfunction: comparison of resting scintigraphy with 201-Tl and 99m-Tc-sestamibi. *Circulation* 1994;89:2552–9.
 14. Bellenger NG, Pennell DJ. Ventricular function. In: Manning WJ, Pennell DJ, editors. *Magnetic Resonance in Clinical Cardiology*. New York, NY: Churchill Livingstone, 2002.
 15. Chien D, Edelman R. Ultra fast imaging using gradient echos. *Magn Reson Q* 1991;7:31–56.
 16. Garot J, Bluemke DA, Osman NF, et al. Transmural contractile reserve after reperfused myocardial infarction in dogs. *J Am Coll Cardiol* 2000;36:2339–46.
 17. Wijns W, Vatner SF, Camici PG. Hibernating myocardium. *N Engl J Med* 1998;339:173–81.
 18. Myers JH, Stirling MC, Choy M, Buda AJ, Gallagher KP. Direct measurement of inner and outer wall thickening dynamics with epicardial echocardiography. *Circulation* 1986;74:164–72.
 19. Gallagher KP, Osakada G, Matsuzaki M, Miller M, Kemper WS, Ross J, Jr. Nonuniformity of inner and outer systolic wall thickening in conscious dogs. *Am J Physiol* 1985;249:H241–8.
 20. Wu E, Judd RM, Vargas JD, Klocke FJ, Bonow RO, Kim RJ. Visualisation of presence, location, and transmural extent of healed Q-wave and non-Q-wave myocardial infarction. *Lancet* 2001;357:21–8.
 21. van der Wall EE, Vliegen HW, de Roos A, Bruschke AVG. Magnetic resonance imaging in coronary artery disease. *Circulation* 1995;92:2723–39.
 22. van der Geest RJ, Reiber JH. Quantification in cardiac MRI. *J Magn Reson Imaging* 1999;10:602–8.
 23. Wagner A, Mahrholdt H, Holly TA, et al. Contrast-enhanced MRI and routine single photon emission computed tomography (SPECT) perfusion imaging for detection of subendocardial myocardial infarcts: an imaging study. *Lancet* 2003;361:374–9.
 24. Pasquet A, Robert A, D'Hondt AM, Dion R, Melin JA, Vanoverschelde JL. Prognostic value of myocardial ischemia and viability in patients with chronic left ventricular ischemic dysfunction. *Circulation* 1999;100:141–8.
 25. Lancellotti P, Benoit T, Rigo P, Pierard LA. Dobutamine stress echocardiography versus quantitative technetium-99m sestamibi SPECT for detecting residual stenosis and multivessel disease after myocardial infarction. *Heart* 2001;86:510–5.
 26. King DL, Harrison MR, King DL, Jr., Gopal AS, Martin RP, DeMaria AN. Improved reproducibility of left atrial and left ventricular measurements by guided three-dimensional echocardiography. *J Am Coll Cardiol* 1992;20:1228–45.
 27. Panza JA, Dilsizian V, Laurienzo JM, Curiel RV, Katsiyannis PT. Relation between thallium uptake and contractile response to dobutamine: implications regarding myocardial viability in patients with chronic coronary artery disease and left ventricular dysfunction. *Circulation* 1995;91:990–8.
 28. Bax JJ, Visser FC, Poldermans D, et al. Time course of functional recovery of stunned and hibernating segments after surgical revascularization. *Circulation* 2001;104:1314–8.
 29. Frangogiannis NG, Shimoni S, Chang S, et al. Active interstitial remodeling: an important process in the hibernating human myocardium. *J Am Coll Cardiol* 2003;39:1468–74.
 30. Kim RJ, Fieno DS, Parrish TB, et al. Relationship of MRI delayed contrast enhancement to irreversible injury, infarct age, and contractile function. *Circulation* 1999;100:1992–2002.
 31. Reimer KA, Jennings RB. The changing anatomic reference base of evolving myocardial infarction: underestimation of myocardial collateral blood flow and overestimation of experimental anatomic infarct size due to tissue edema, hemorrhage and acute inflammation. *Circulation* 1979;60:866–76.

Impact of scar thickness on the assessment of viability using dobutamine echocardiography and thallium single-photon emission computed tomography: A comparison with contrast-enhanced magnetic resonance imaging

Charles Nelson, Jane McCrohon, Frederick Khafagi, Stephen Rose, Rodel Leano, and Thomas H. Marwick

J. Am. Coll. Cardiol. 2004;43;1248-1256

doi:10.1016/j.jacc.2003.09.062

This information is current as of April 8, 2011

Updated Information & Services	including high-resolution figures, can be found at: http://content.onlinejacc.org/cgi/content/full/43/7/1248
References	This article cites 27 articles, 18 of which you can access for free at: http://content.onlinejacc.org/cgi/content/full/43/7/1248#BIBL
Citations	This article has been cited by 9 HighWire-hosted articles: http://content.onlinejacc.org/cgi/content/full/43/7/1248#otherarticles
Rights & Permissions	Information about reproducing this article in parts (figures, tables) or in its entirety can be found online at: http://content.onlinejacc.org/misc/permissions.dtl
Reprints	Information about ordering reprints can be found online: http://content.onlinejacc.org/misc/reprints.dtl